INSTITUTE OF PHYSICS PUBLISHING PHYSICS IN MEDICINE AND BIOLOGY

Phys. Med. Biol. **47** (2002) N133–N143 PII: S0031-9155(02)32395-9

NOTE

Investigation of photon beam output factors for conformal radiation therapy—Monte Carlo simulations and measurements

F Haryanto[1], M Fippel[1], W Laub[2], O Dohm[1] and F Nüsslin[1]

[1] Abteilung für Medizinische Physik, Radioonkologische Universitätsklinik, Hoppe-Seyler-Str.3, 72076 Tübingen, Germany
[2] Department of Radiation Oncology, William Beaumont Hospital, Royal Oak, MI 48073-6769, USA

Received 7 January 2002, in final form 18 March 2002
Published 22 May 2002
Online at stacks.iop.org/PMB/47/N133

Abstract

The purpose of this study was to investigate beam output factors (OFs) for conformal radiation therapy and to compare the OFs measured with different detectors with those simulated with Monte Carlo methods. Four different detectors (diode, diamond, pinpoint and ionization chamber) were used to measure photon beam OFs in a water phantom at a depth of 10 cm with a source–surface distance (SSD) of 100 cm. Square fields with widths ranging from 1 cm to 15 cm were observed; the OF for the different field sizes was normalized to that measured at a 5 cm × 5 cm field size at a depth of 10 cm. The BEAM/EGS4 program was used to simulate the exact geometry of a 6 MV photon beam generated by the linear accelerator, and the DOSXYZ-code was implemented to calculate the OFs for all field sizes. Two resolutions (0.1 cm and 0.5 cm voxel size) were chosen here. In addition, to model the detector four kinds of material, water, air, graphite or silicon, were placed in the corresponding voxels.

Profiles and depth dose distributions resulting from the simulation show good agreement with the measurements. Deviations of less than 2% can be observed. The OF measured with different detectors in water vary by more than 35% for 1 cm × 1 cm fields. This result can also be found for the simulated OF with different voxel sizes and materials. For field sizes of at least 2 cm × 2 cm the deviations between all measurements and simulations are below 3%. This demonstrates that very small fields have a bad effect on dosimetric accuracy and precision. Finally, Monte Carlo methods can be significant in determining the OF for small fields.

1. Introduction

Since conformal radiation treatment planning has been implemented into the clinical routine, irregular and small fields are often applied in addition to regular fields. Several new approaches have been developed which combine very small fields with irregular fields using static or dynamic techniques (Sharp *et al* 2000, Webb 2001). With recent technologies implemented in and around linear accelerators, they can be realized clinically. But at the same time a lot of inaccuracies in dosimetry and dose calculation also appear.

For small fields where a lack of electron equilibrium and high dose gradients are present, the photon beam output factors (OFs) are difficult to measure and have to be determined with analytical/empirical dose calculations. Measured OF depends on the effective volume of the detector, because electronic disequilibrium happens if half of the field size is smaller than the mean lateral component of the range of the secondary electrons in water.

Many researchers have reported the advantages and disadvantages of detectors that can be used for OF measurements, especially for radiosurgery where the field diameter at isocentre distance ranges typically from 5 mm to 40 mm (De Vlamynck *et al* 1999, Heydarian *et al* 1996, Martens *et al* 2000, Somigliana *et al* 1999, Verhaegen *et al* 1998, Westermark *et al* 2000, Zhu *et al* 2000). Most of their results show that diamond and diode detectors are more reliable than other detectors for measurements of small fields. The diamond detector has good water equivalence and high spatial resolution, but it is expensive and its reading depends on the dose rate and therefore on the measurement depth also (Laub *et al* 1997). With an increasing dose rate, the diamond detector has an under-response. The decrease in the detector's response is a consequence of the very short electron–hole recombination time and this phenomenon is predicted by the theory of radiation-induced conductivity in an insulator (Hoban *et al* 1994, Laub *et al* 1997). The advantages of the diode detector include high spatial resolution, linear dose response, ease of use, and the fact that it requires no bias. On the other hand, this detector is not water-equivalent and has an energy-dependent response, although for relative measurements of small fields this energy-dependent response is not significant. The diode response to the accumulated dose and temperature depends on the doping level in a diode detector. A diode detector with a high doping level can be shown to remain linear after high irradiation doses of high-energy photons, electrons and protons (Rikner and Grusell 1987). To take advantage of this effect, the diode detector was pre-irradiated before it was used for measurement.

In dose calculation, two methods exist, namely superposition/convolution and Monte Carlo, that accurately predict the OFs of linear accelerators for small fields, since both methods account for electron transport (Ahnesjö *et al* 1989, Chetty *et al* 2000, De Vlamynck *et al* 1999, Fix *et al* 2000, Kapur *et al* 1998, Mackie *et al* 1985, van der Zee *et al* 1999, Yu *et al* 1995). Superposition/convolution needs energy kernels, which can be extracted from measurements or can be pre-calculated by Monte Carlo (MC) simulations. This prerequisite is one disadvantage of the method. Furthermore, superposition/convolution does not account for the secondary electron disequilibrium in the presence of inhomogeneities. The rapid evolution in computer technologies and new adapted MC methods, on the other hand, reduce the computing time of these methods, and can thereby realize their usage in clinical routines feasible in the future.

The above discussion motivates measurement of OFs with different types of detectors and simulation of these measurements with MC methods. In this work, the capability of an ionization chamber, a pinpoint ion chamber, a diamond detector, and a diode detector to measure OFs for small fields was compared and was verified with MC methods. The MC simulation was divided into two parts. First, the BEAM code system (Roger *et al* 1995)

was used to model the linear accelerator head. Then, using the phase space file which was produced from the model, the particle transport in a water phantom was simulated. For these simulations, the DOSXYZ code was used.

2. Materials and methods

2.1. Measurements

The largest sensitive volume of a detector used in this work is 0.125 cm^3 and belongs to an ionization chamber (PTW-Freiburg, type 31002). In contrast to that, a diode detector shows the smallest sensitive volume. It has a disc-like shape with a 1 mm^2 surface area and a thickness of 2.5 μm (PTW-Freiburg, type 60008). The diamond detector (PTW-Freiburg, type 60003) should also act as a suitable detector because of its small sensitive volume (5.6 mm^2 surface area and 0.25 mm thickness). The last one of the detectors used here was a pinpoint thimble chamber (PTW-Freiburg, type 31006) with a sensitive volume of 2 mm in diameter and 5 mm in length. All detectors were used to measure OFs. Profiles and depth dose distributions were measured with all but the pinpoint chamber.

An Elekta Sl*i* plus linear accelerator equipped with multileaf collimators (MLC) was used for the measurements with 6 MV photon beams. All measurements were performed in a MP3 water phantom (PTW-Freiburg). Profile and depth dose distribution measurements were performed at 90 cm SSD and 10 cm $\times$ 10 cm field size. Detectors were connected to the MP3 dual channel. The detector orientation was set to give the maximum spatial resolution in the x-direction for profile measurements and in the z-direction for depth dose measurements.

The OF was determined as a ratio of the measured data for a certain field size and the measured data for a reference field size. In this study our focus is on small field sizes; therefore the 5 cm $\times$ 5 cm field was chosen as a reference field. The OFs were measured with an Unidos Universal Dosimeter (PTW-Freiburg), the surface of the water phantom was set to 100 cm SSD and the accelerator was set to apply 100 monitor units (MU) per minute for all fields. Each detector was placed 10 cm below the water surface and was oriented for maximum spatial resolution. The orientation of the pinpoint chamber axis was perpendicular to the beam axis. Square fields were chosen and the field widths varied from 1 cm to 15 cm. In addition, the OFs for 10 cm $\times$ 10 cm and 5 cm $\times$ 5 cm fields at off-set (leaf direction) -10 cm, -5 cm, 5 cm and 10 cm were measured with the ionization chamber.

2.2. Accelerator model

The accelerator model was accomplished in two stages using the BEAM/EGS4 program (Nelson *et al* 1985, Roger *et al* 1995). The first stage begins at the target and includes primary collimator, low secondary filter, monitor chamber, mirror and anti-backscattering plate. The phase space data generated from this stage were universal for all field sizes, and were taken as input for the second stage of the simulation. To score about 1×10^8 particles in the first phase space, 1×10^7 electrons on the first stage were simulated. In the second stage, all other components of the linear accelerator, MLC, back-up jaws and jaws, were modelled. MLC and back-up jaws have rounded ends. For both components, the existing component module MCLQ was used. From this stage, the secondary phase space data were scored in air at a 90 cm or 100 cm distance from the electron target and were used as a source for the simulations of particles in the water phantom. Each particle from the first phase space data was re-used three times to produce the second phase space data. The size of these phase data depends on the field size: the larger the field size, the larger the size of the phase space produced by the

simulation (e.g. 9×10^4 particles for a 1 cm $\times$1 cm field and 3×10^7 particles for a 15 cm $\times$ 15 cm field). Almost all components of the linear accelerator head were modelled, except the exit window. The exit window does not have a significant effect on the photon beam due to its material and dimension (very thin layer).

The incident electron source striking the target was modelled as a point source and the diameter of the electron beam spot at the target was 2 mm (Elekta). This point source has a Gaussian spectrum and was located 3 cm above the target. The mean energy of this spectrum was 6.8 MeV with a full width half maximum energy spread of 1.0 MeV (Elekta). To obtain the mean energy of this spectrum, a trial and error method was used, until good agreement between calculated depth dose and measured depth dose was achieved.

To improve the efficiency of the simulations, bremsstrahlung photon splitting was implemented on the first stage. Each bremsstrahlung event produced 25 photons, all of which have equal weight. The energy cut-off parameters used were ECUT = AE = 700 keV and PCUT = AP = 10 keV. The PRESTA algorithm was used.

2.3. Simulations in the water phantom

The DOSXYZ code was employed to simulate particle transport in the water phantom (Ma *et al* 1996). This code is based on 3D Cartesian coordinates. To verify the accelerator model, profile and depth dose distributions were separately calculated while keeping the computer calculation time as low as possible. Depth dose distributions were calculated in a 1 cm $\times$ 1 cm area around the central axis with thickness varying from 0.2 cm at the build-up region to 1 cm at other regions. The resolution of the voxels in the penumbra region of the profiles was 0.1 cm.

OF calculations were performed using this code with resolutions (voxel sizes) of 0.1 cm and 0.5 cm. The OF for a given field size was calculated in the same way as described for the measurements. The number of particle histories in the first stage for each field size was set to be equal; therefore, the monitor chamber received the same amount of radiation. This is valid, if the number of backscattered radiation particles into the monitor chamber originating from the MLCs and jaws is negligible. For the Elekta Sl*i* plus this was found to be a good assumption, since the machine is equipped with an anti-backscattering plate. Hounsell (1998) has investigated the effect of anti-backscatter on an Elekta linear accelerator. His work showed that backscatter radiation can be neglected due to the presence of this plate. The number of particle histories in the simulations of the water phantom varies with field size.

Another aspect, the water equivalence of the detectors, was investigated using the detector material, air, silicon and graphite. These materials were placed in the corresponding voxels to model the detector. Silicon was used as the material for the diode detector, air represented the material for the ionization chamber and carbon, with a density of 2.26 g cm^{-3}, was employed as an approximation for the diamond detector. The presence of an air cavity in water caused an increase in the calculation time by a factor of five because more histories were needed to calculate the ionization chamber response with reasonable statistical uncertainty.

3. Results and discussion

3.1. Output factor measurements

Figure 1 presents the results of the OF measurements with the different detectors. For all field sizes between 2 cm $\times$ 2 cm and 15 cm $\times$ 15 cm the results of the measurements show good agreement within 3%. The results of the OF measurements for the 1 cm $\times$ 1 cm field, on the other hand, show much larger variations, the largest difference observed between the OF

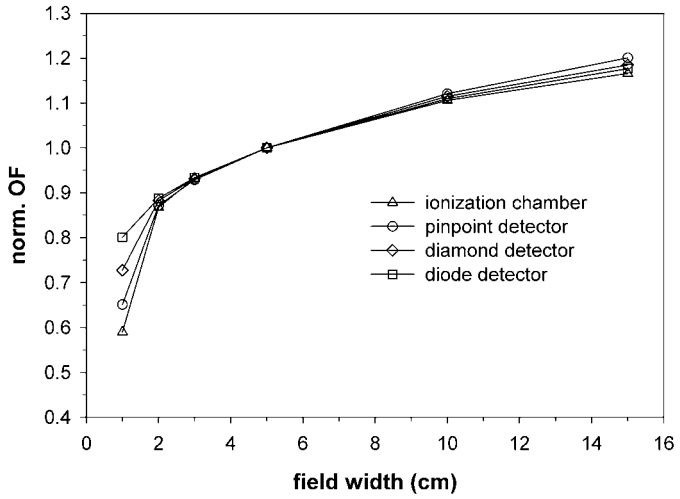

Figure 1. OFs measured with four detectors. Triangles: ionization chamber; circles: pinpoint detector; diamonds: diamond detector; squares: diode detector.

measured with the diode detector and the ionization chamber was found to be about 35%. There are two aspects that cause large differences for this field. Both are related to the presence of the lateral electronic disequilibrium in small fields. The first aspect is the detector size (a larger detector size would reduce the OF measured for small fields). The second aspect is the water equivalence of the detector material.

Comparisons of ionization chamber and pinpoint chamber measurements show that the size of the air cavity is the most important aspect for detectors that have an air cavity. The larger the size of the air cavity, the more the lateral electronic disequilibrium increases, and a lower dose results for the air within the cavity compared to the case with tissue (water) at the same position. Larger air cavities may further reduce the relative dose reading of detectors. Moreover, the relative dose reading of the detector is also reduced because the detector averages the dose across its sensitive volume. The measured OF with the pinpoint chamber for the largest fields is slightly higher due to the over-response of this detector to low-energy scatter (Martens *et al* 2000). For the 15 cm $\times$ 15 cm field the response of the pinpoint chamber is 3.0% higher than that measured with the ionization chamber.

The effect of tissue equivalence can be investigated on the OF measured with a diamond detector and a diode detector. For small fields, the OF measured with the diode detector, which is non-water-equivalent, is larger than the OF measured with the water-equivalent diamond detector. There are two reasons for this phenomenon (Somigliana *et al* 1999): first, the material surrounding the diode detector reduces lateral electronic disequilibrium, because it increases the lateral scattering. Second, the secondary electrons play an important role in small fields. If the field width here is less than the maximum range of the secondary electrons, the average electron energy spectrum at the central axis increases due to the lack of lateral electronic equilibrium. For secondary electrons produced by a 6 MV x-ray beam the electron mass collision stopping power ratio between water and silicon indicates a slight decrease as the electron energy increases. This is the reason why the OF measured for small fields is slightly overestimated.

All measured OFs show the same sharp drop for a 2 cm $\times$ 2 cm field size. This behaviour of the measured OFs is correlated with the size of electron source. Zhu and Bjärngard (1994)

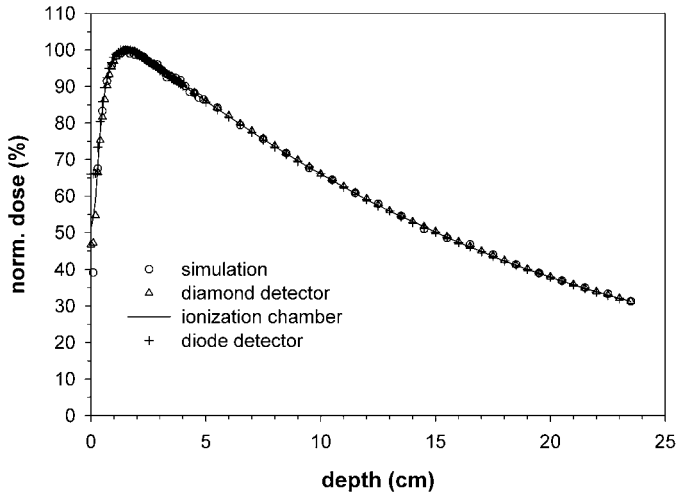

Figure 2. Comparison of depth dose distributions measured with three types of detectors and calculated with Monte Carlo methods. Circles: simulation; triangles: diamond detector; solid line: ionization chamber; plus: diode detector.

reported that the shape of measured OFs for field sizes less than 3 cm × 3 cm is determined by physical effects other than photon scatter.

3.2. Verification of the accelerator model

Figure 2 shows the depth dose distributions measured and calculated for a 10 cm × 10 cm field. It can be seen from this figure that the curves measured with the diode detector and the ionization chamber agree well with the curve calculated using Monte Carlo methods. This proves that the diode detector responds linearly to dose rate. This result differs from the findings of other researchers. They reported that there is some depth-dependent under-response in diode depth dose distributions due to the response supralinearity with dose rate (Heydarian *et al* 1996). The different manufacturers that produced the detectors can be a good reason for the differences found in this work, because the characteristics of the diode detector depend on the doping level in the diode detector. The diode detector used here was set up to give the same results as the ionization chamber for percentage depth dose measurements. Figure 2 does not indicate the sublinearity of the diamond detector response with the dose rate, because this effect has been removed by correcting the measured values. This correction was taken from the work of Laub *et al* (1997). The good agreement between the depth dose distributions measured and calculated within 2% confirms the validity of the electron spectrum that was employed for the simulation of the linear accelerator. In this calculation, the statistical uncertainty was kept within 1%.

A comparison of the measured and calculated profiles for the 10 cm × 10 cm field at maximum depth (1.5 cm) can be found in figure 3. Good agreement within 2% between calculated and measured profiles with the diamond and the diode detector was achieved. The largest deviations between the calculated and measured profiles using the ionization chamber were found in the penumbra region. This is mainly due to the larger size of the sensitive volume of the ionization chamber. The statistical uncertainty of the calculated profiles was kept within 1%. The profile measurements were affected by different factors, namely the finite size of the detector, the change of the electron transport within the detector, the detector energy and dose rate dependencies (Heydarian *et al* 1996).

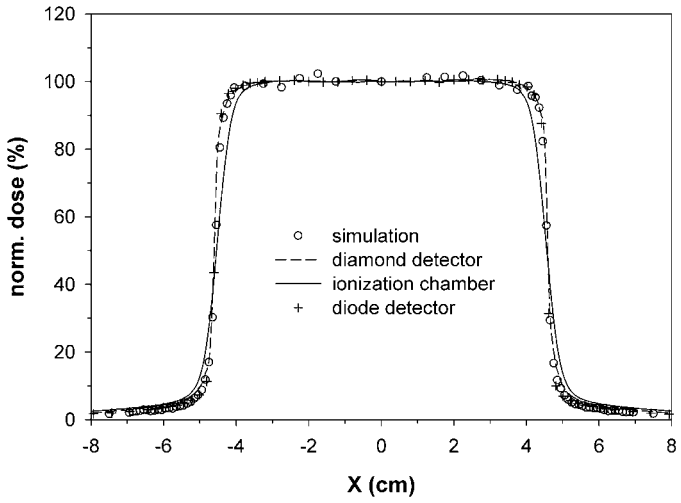

Figure 3. Comparison of a profile measured with three types of detectors and calculated with Monte Carlo methods. Circles: simulation; dashed line: diamond detector; solid line: ionization chamber; plus: diode detector.

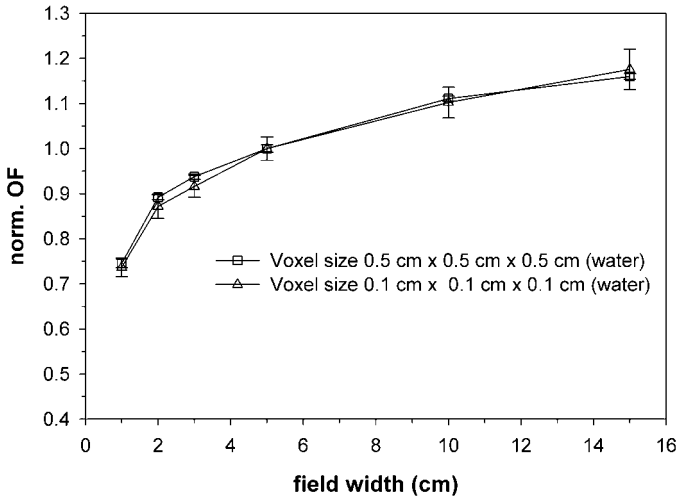

Figure 4. OFs calculated with two different voxel sizes. Squares: 0.5 cm × 0.5 cm × 0.5 cm voxel size; triangles: 0.1 cm × 0.1 cm × 0.1 cm voxel size.

3.3. Output factor comparisons

The results of the OF calculations with different voxel sizes are shown in figure 4. From this figure, it can be seen that voxel size affect the standard error of calculation, because the number of particles that interact in this voxel decreases with decreasing voxel size. The value of the OF calculated with 1 mm voxel size for the 15 cm × 15 cm field has statistical uncertainty within 4.5%.

From figure 5, it can be seen that the OFs measured with the diamond and the diode detector and those calculated with 0.1 cm voxel size are in good agreement (within 2%) with a 2 cm × 2 cm field size. For the 1 cm × 1 cm field, the difference between the measured OF

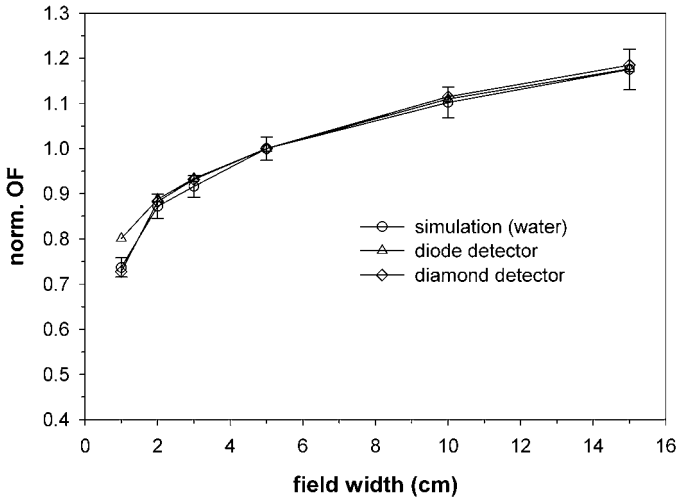

Figure 5. Comparison of OFs measured with a diamond detector (diamonds) and a diode detector (triangles), and calculated with 0.1 cm × 0.1 cm × 0.1 cm voxel size (circles).

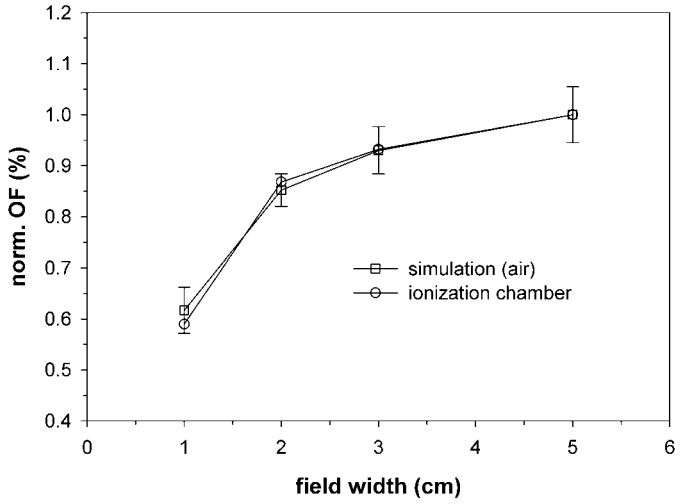

Figure 6. Comparison of OFs measured with an ionization chamber (circles) and calculated with 0.5 cm × 0.5 cm × 0.5 cm voxel size and air as material (squares).

with the diamond detector and the calculated OF is smaller than the difference between that measured and calculated with the diode detector. It indicates that the water equivalence of the diamond detector material is better than that of the diode detector. By comparing figures 5 and 8, the effect of the water equivalence of the detectors can be evaluated. If we replace the material of the detector voxel by the material of the diode detector, good agreement between measured and calculated OFs was also found for the 1 cm × 1 cm field.

In figure 6 the OFs measured with the ionization chamber and those calculated with air as the material of the voxels that describe the sensitive volume of the ionization chamber are presented. The 0.5 cm voxel size was chosen because this represents the sensitive volume of the ionization chamber (0.125 cm^3). From this figure it can be seen that the effect of the material for the voxel plays an important role for calculated OFs. Due to the presence of an air

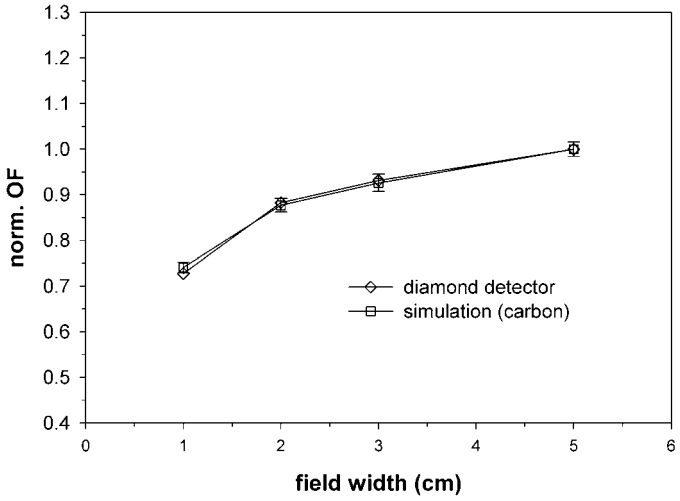

Figure 7. Comparison of OFs measured with a diamond detector (diamonds) and calculated with 0.1 cm × 0.1 cm × 0.1 cm voxel size and carbon as material (squares).

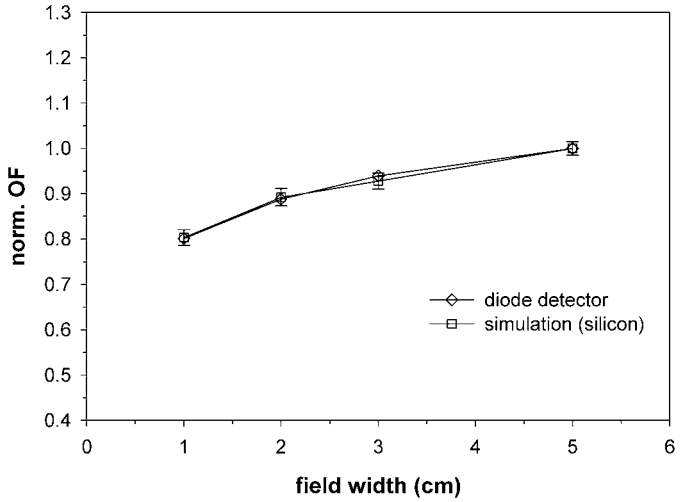

Figure 8. Comparison of OFs measured with a diode detector (diamonds) and calculated with 0.1 cm × 0.1 cm × 0.1 cm voxel size and silicon as material (squares).

cavity in water the statistical uncertainties of calculation are larger. The agreement between the calculated OFs and those measured with the ionization chamber for all fields was found to be better than 3%. The same phenomenon can be seen in figures 7 and 8. Figure 7 shows the OFs measured with the diamond detector and those calculated with carbon as the material of the voxel, and in figure 8 a comparison of the OFs measured with the diode detector and those calculated with silicon as the material of the voxel can be seen.

Figure 9 compares the OFs measured with the ionization chamber and those calculated with 0.5 cm voxel size for off-axis fields. Good agreement within 2% was found in this comparison. Therefore, the low secondary filter was correctly modelled, because the design of this filter plays a role in the variation of the accelerator output as a function of the off-set fields.

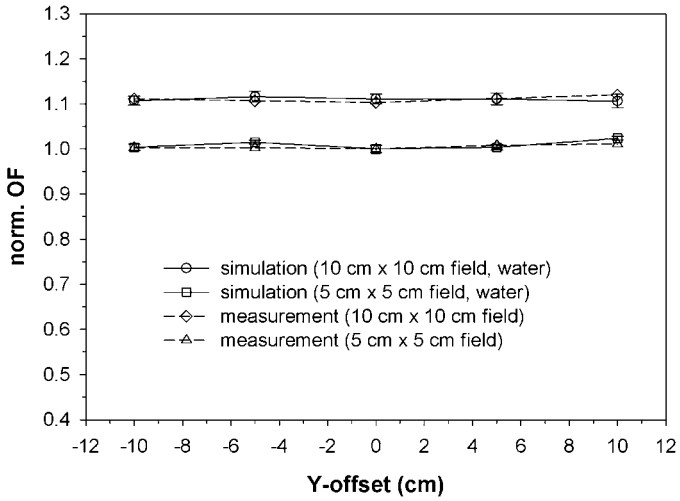

Figure 9. Comparison of OFs measured with an ionization chamber and calculated with 0.5 cm × 0.5 cm × 0.5 cm voxel size for off-axis fields. Circle and solid line: simulation (10 cm × 10 cm field); squares and solid line: simulation (5 cm × 5 cm field); diamonds and dashed line: measurement (10 cm × 10 cm field); triangles and dashed line: measurement (5 cm × 5 cm field).

4. Conclusions

The result of OF measurements for field sizes of at least 2 cm × 2 cm does not depend on the detector type used. Only for 1 cm × 1 cm fields are there effects that are characteristic of some detectors and affect the measurements. In OF calculation, not only does the voxel size play an important role for the 1 cm × 1 cm field, but so does the material of the voxels that describes the volume of the detector. Both, voxel size and detector material give no significant difference for field sizes equal to or larger than 2 cm × 2 cm.

One result of this study is that the lack of lateral electronic equilibrium can cause errors in dose calculations, especially in OF calculation for small fields. However, if we replace the voxel material by the detector material and if we use voxel sizes comparable to the detector sizes, good agreement between the measured and the calculated OFs can be achieved. It is difficult to decide which type of detector gives the proper OF for small fields. The ionization chamber can be ignored for fields smaller than 2 cm × 2 cm due to its sensitive volume. The diamond detector can be considered to give better results due to its small sensitive volume and its water equivalence.

Finally, Monte Carlo methods give results that can be seen as results for an ideal linear accelerator and can be significant in determining the correct OF for small fields. The material of the voxel should be considered during the simulations to give better agreement between calculation and measurement.

Acknowledgments

One of the authors (F Haryanto) was kindly given a grant by the German Academic Exchange Service (Deutscher Akademischer Austausch-Dienst). The support to this investigation given partly by the Deutsche Krebshilfe and partly by the research funding program *Fortune* of the Tuebingen University Hospital is gratefully acknowledged. The authors would also like to thank the referees for their comments.

References

Ahnesjö A, Andreo P and Brahme A 1989 Collapsed cone convolution of radiant energy for dose calculation in heterogeneous media *Med. Phys.* **16** 577–92

Chetty I, DeMarco J J and Solberg T D 2000 A virtual source model for Monte Carlo modeling of arbitrary intensity distributions *Med. Phys.* **27** 166–72

De Vlamynck K, Palmans H, Verhaegen F, Wagter C De, Neve W De and Threirens H 1999 Dose measurements compared with Monte Carlo simulations of narrow 6 MV multileaf collimator shaped photon beams *Med. Phys.* **26** 1874–82

Fix M K, Keller H and Rüegsegger P 2000 Simple beam models for Monte Carlo photon beam dose calculations in radiotherapy *Med. Phys.* **27** 2739–47

Heydarian M, Hoban P W and Beddoe A H 1996 A comparison of dosimetry techniques in stereotactic radiosurgery *Phys. Med. Biol.* **41** 93–110

Hoban P W, Heydarian M, Beckham W A and Beddoe A H 1994 Dose rate dependence of a PTW diamond detector in dosimetry of a 6 MV photon beam *Phys. Med. Biol.* **39** 1219–29

Hounsell A R 1998 Monitor chamber backscatter for intensity modulated radiation therapy using multileaf collimators *Phys. Med. Biol.* **43** 445–54

Kapur A, Ma C-M, Mok Ed C, Findley D O and Boyer A L 1998 Monte Carlo calculations of electron beam output factors for a medical linear accelerator *Phys. Med. Biol.* **43** 3479–94

Laub W U, Kaulich T W and Nüsslin F 1997 Energy and dose rate dependence of a diamond detector in the dosimetry of 4–25 MV photon beams *Med. Phys.* **24** 535–6

Ma C-M, Reckwerdt P, Holmes M, Rogers D W O, Geiser B and Walters B 1996 DOSXYZ User's Manual *National Research Center of Canada Report* PIRS-0509B

Mackie T R, Scrimger J W and Battista J J 1985 A convolution method of calculating dose for 15-MV x rays *Med. Phys.* **12** 188–96

Martens C, Wagter C De and Neve W De 2000 The value of the pinpoint ion chamber for characterization of small field segments used in intensity-modulated radiotherapy *Phys. Med. Biol.* **45** 2519–30

Nelson W R, Hirayama H and Rogers D W O 1985 The EGS4 Code System *SLAC Report* No SLAC-265

Rikner G and Grusell E 1987 General specifications for silicon semiconductors for use in radiation dosimetry *Phys. Med. Biol.* **32** 1109–17

Roger D W O, Faddegon B A, Ding G X, Ma C-M, Wie J and Mackie T R 1995 BEAM: a Monte Carlo code to simulate radiotherapy treatment units *Med. Phys.* **22** 503–24

Sharpe M B, Miller B M, Yan D and Wong J W 2000 Monitor unit settings for intensity modulated beams delivered using a step-and-shoot approach *Med. Phys.* **27** 2719–25

Somigliana A *et al* 1999 Dosimetry of gamma knife and linac-based radiosurgery using radiochromic and diode detectors *Phys. Med. Biol.* **44** 887–97

Webb S 2001 Concepts for shuttling multileaf collimators for intensity-modulated radiation therapy *Phys. Med. Biol.* **46** 637–51

Westermark M, Arndt J, Nilsson B and Brahme A 2000 Comparative dosimetry in narrow high-energy photon beams *Phys. Med. Biol.* **45** 685–702

van der Zee W and Wellewerd J 1999 Calculating photon beam characteristics with Monte Carlo technique *Med. Phys.* **26** 1883–92

Verhaegen F, Das I J and Palmans H 1998 Monte Carlo dosimetry study of a 6 MV stereotactic radiosurgery unit *Phys. Med. Biol.* **43** 2755–68

Yu C X, Mackie T R and Wong J W 1995 Photon dose calculation incorporating explicit electron transport *Med. Phys.* **22** 1157–65

Zhu T C and Bjärngard B E 1994 head-scatter factor for small field sizes *Med. Phys.* **21** 65–8

Zhu X R, Allen J J, Shi J and Simon W E 2000 Total scatter factors and tissue maximum ratios for small radiosurgery fields: comparison of diode detectors, a parallel-plate ion chamber and radiographic film *Med. Phys.* **27** 472–7